The effect of jet velocity profile on the characteristics of thickness and velocity of the liquid sheet formed by two impinging jets

Y. J. Choo[a)]
Korea Atomic Energy Research Institute, 105, Yuseong-Gu, Daejeon, 305-600, Korea

B. S. Kang[b)]
Department of Mechanical Engineering, Chonnam National University, 300, Yongbong-Dong, Buk-Gu, Gwangju, 500-757, Korea

(Received 17 April 2007; accepted 6 September 2007; published online 9 November 2007)

In this study, the effect of jet velocity profile on the thickness and velocity of the liquid sheet formed by two low-speed impinging jets was investigated. In addition to the constant jet velocity and the Poiseuille parabolic profile, the jet velocity profile measured experimentally was considered to account for the real nonuniform jet velocity profile. For three jet velocity profiles, the distributions of the thickness and velocity of the liquid sheet were analytically predicted by solving conservation equations for mass, momentum, and energy. The predicted results were compared with the previous experimental results. The jet velocity profile affected the resulting thickness and velocity characteristics of the liquid sheet. The distributions of the thickness and velocity of the liquid sheet predicted by using the measured jet velocity profile produced more acceptable results, which agreed better with the experimental observations, than those obtained by using the constant jet velocity, which has been commonly used in previous theoretical works. © *2007 American Institute of Physics*. [DOI: 10.1063/1.2795780]

I. INTRODUCTION

Impinging-jet injectors, which are commonly used in liquid propellant rocket engines, atomize liquid propellants (fuel and oxidizer) by the impingement (one upon the other) of two identical and cylindrical jets at high liquid jet velocities.[1] Two impinging jets at low liquid jet velocities in turn produce a leaf-shaped, expanding sheet normal to the plane of the two liquid jets, as shown in Fig. 1. Several investigations on the liquid sheet formed by low-speed impinging jets have been conducted over the years. Previous analytical studies have included the modeling of the thickness,[2–6] shape,[4–7] and velocity[6] of the liquid sheet, as well as the size of the droplets detaching from the rim of the liquid sheet.[8] Some experimental studies have also focused on the thickness,[9–12] shape,[5–7,9,13] and velocity[13–15] of the liquid sheet and on the droplet size.[6,7]

The velocity distribution of the liquid sheet is closely related to the direction of motion and the kinetic energy of the droplets disintegrating from the liquid sheet. It also plays an important role in the modeling analyses of liquid sheet disintegration. For example, the velocity of the liquid sheet relative to the surrounding air is a very important factor in well-known disintegration mechanisms of liquid sheets, such as the perforation breakup model and the aerodynamic wave breakup model. The size distribution of liquid droplets detaching from the rim of the liquid sheet depends on the thickness and orientation of the rim. Therefore, fundamental studies on the characteristics of the thickness and velocity of the liquid sheet are vital because the information obtained from such studies can be used to predict the characteristics of the droplets formed.

In many previous analytical studies on the prediction of sheet thickness and the size of the disintegrating droplets, the liquid sheet velocity has long been assumed equal to the jet velocity U or the axial component of the jet velocity $U\cos\theta$ and independent of the angular position. For example, Taylor[9] considered that the sheet velocity was the same as that of the jet because there was no means by which energy could be absorbed. Using high-speed cinematography, Dombrowski and Hooper[14] measured the local sheet velocity at the axis of the sheet by measuring the distances traveled by surface irregularities and waves. For laminar jets at low impingement angles, a high-velocity stream existing in the jets moves along the axis of the sheet resulting in a sheet velocity higher than the mean jet velocity. For high impingement angles or for turbulent jets, the sheet velocity is lower than the jet velocity because the high-velocity stream is more evenly distributed on the sheet. Choo and Kang[15] directly measured the local velocities of the liquid sheet using a laser instrument. It was shown that the local sheet velocities were higher than the mean jet velocity with the exception of the lowest velocities near the edge of the sheet; this result contradicted the findings of earlier studies, in which the sheet velocity was assumed equal to or less than the jet velocity. It was also pointed out that the velocity profile across the preimpinging jet greatly affected the sheet velocity distribution. A similar method adopted by Dombrowski and Hooper[14] was used by Li and Ashgriz[13] who verified that the sheet velocity decreased with increasing azimuthal angle; this phenomenon was also observed by Choo and Kang.[15]

There have been several theoretical modeling efforts for

[a)]Electronic mail: chooyj@kaeri.re.kr
[b)]Electronic mail: bskang@chonnam.ac.kr

 © 2007 American Institute of Physics

Downloaded 11 Nov 2007 to 168.131.132.191. Redistribution subject to AIP license or copyright, see http://pof.aip.org/pof/copyright.jsp

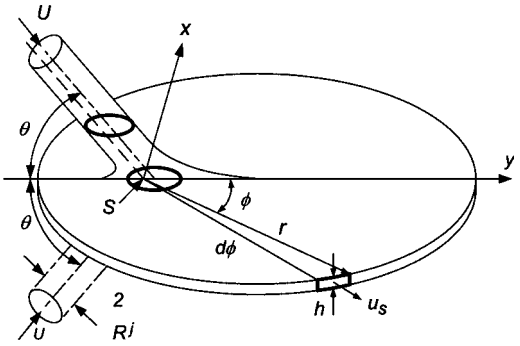

FIG. 1. A liquid sheet formed by two impinging jets at low jet velocity U with jet radius R_j and impingement angle 2θ [modified from Hasson and Peck (Ref. 4)].

the sheet thickness. Taylor[9] provided theoretical and experimental explanations that stated that the thickness h at any point on the liquid sheet is inversely proportional to the radius r, which is the distance from the impingement point. This relationship is expressed as

$$h = \frac{K(\phi,\theta)}{r}, \tag{1}$$

where a proportionality constant K is defined as the liquid sheet thickness parameter. This relationship has been used in all succeeding analytical studies. Ranz[2] and Miller[3] used the principle of conservation of mass and momentum to obtain the thickness distribution. Hasson and Peck[4] assumed that the jet in a plane parallel to the liquid sheet takes the shape of an ellipse, and that mass and momentum are conserved between an angular element in the ellipse and the corresponding element in the liquid sheet. Ibrahim and Przekwas[5] adopted the expression for the initial sheet thickness obtained by Naber and Reitz[16] in their study of the engine spray/wall impingement. All the preceding theoretical expressions for the sheet thickness indicate that the sheet thickness is related only to the orifice diameter, impingement angle, and azimuthal angle, and not to the jet velocity.

Experimental results that can be used to compare with the above theoretical predictions are very scarce. Taylor[9] estimated the sheet thickness by measuring the volume of the liquid passing through a small section of the sheet. Shen and Poulikakos[11] used a nonintrusive holographic technique to measure the thickness of the whole liquid sheet. Choo and Kang[12] used the interference phenomenon of light to measure the thickness of the liquid sheet. It was shown that the thickness values predicted by all of the previous theoretical models assuming a uniform jet velocity were overestimated at low azimuthal angles and underestimated for the remaining part of the sheet.

Recently, Bremond and Villermaux[6] investigated the shape and thickness of the liquid sheet, the size of the rim in a circular cross section, and the droplets disintegrating from the rim. They insisted that the initial jet velocity profile should be considered in the prediction of the distributions of the thickness and velocity of the liquid sheet. Assuming a Poiseuille parabolic velocity profile of the jets, they predicted the distributions of the thickness and velocity of the

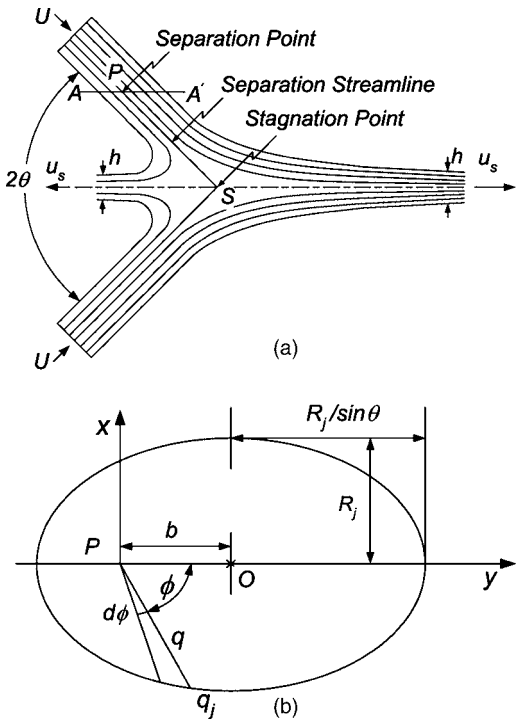

FIG. 2. Sectional views of a liquid sheet and a jet. (a) Streamlines in a section through $\phi=0°$ and $\phi=\pi$. (b) Elliptical cross section AA' of an inclined jet and related parameters.

liquid sheet. However, in real situations, the velocity profile of the jets starts to relax downstream of the exit. The velocity profile of the jets just at the impingement point does not exactly match the Poiseuille parabolic velocity profile, a finding which was already pointed out by Choo and Kang.[15] The jet velocity profile measured at the impingement point deviated from the assumed Poiseuille profile. Therefore, in this study, the effect of the jet velocity profile on the thickness and velocity of the liquid sheet was investigated based on the analysis performed by Bremond and Villermaux.[6] The distributions of the thickness and velocity of the liquid sheet was predicted using the jet velocity profile measured experimentally by Choo and Kang.[15] The predicted results were also compared with the previous experimental results obtained by Choo and Kang.[12,15]

II. THEORETICAL PREDICTIONS

Theoretical prediction taken in this study adopted the analysis performed by Bremond and Villermaux[6] using a Poiseuille parabolic velocity profile.

A. Streamlines and jet cross section

Figure 2(a) shows the streamlines in the vertical cross section of two jets and the sheet shown in Fig. 1 along the y axis. In this kind of free surface flow, the effect of gravity, surface tension, and viscous forces can be neglected in comparison with the inertia force. The impact pressure generated in the area of impact deflects each streamline of the jets into $+y(\phi=0°)$ and $-y(\phi=\pi)$ directions from a stagnation point

Downloaded 11 Nov 2007 to 168.131.132.191. Redistribution subject to AIP license or copyright, see http://pof.aip.org/pof/copyright.jsp

S, as shown in Fig. 2(a). The streamlines in the jets also retain their angular positions in the sheet from the stagnation point.

Figure 2(b) shows an elliptical cross section AA' through the jet in a plane parallel to the sheet having a major axis equal to $2R_j/\sin\theta$ and a minor axis equal to $2R_j$. The distance between the separation point P and the center of the ellipse O is $b=OP$. The points on the ellipse (q_j) can be expressed using the cylindrical coordinate system $q_j=f(q,\phi)$,

$$q_j=\{b\cos\phi\sin^2\theta-[R_j^2(1-\cos^2\phi\cos^2\theta)-b^2\sin^2\phi\sin^2\theta]^{1/2}\}/(1-\cos^2\phi\cos^2\theta). \quad (2)$$

The separation point P coincides with the stagnation point S and the separation streamline PS that intersects the center plane of the sheet is the only streamline of the jet suffering no deflection.

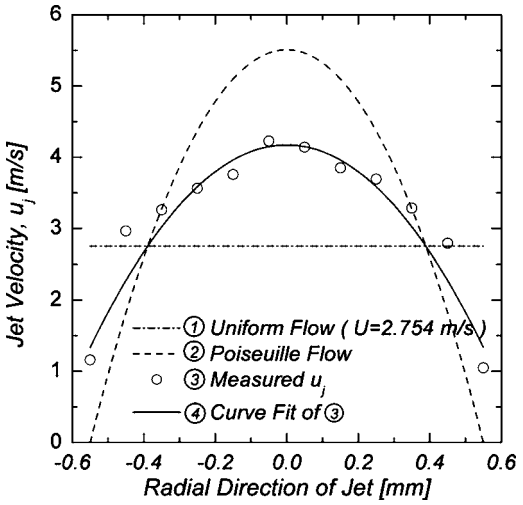

FIG. 3. Jet velocity distributions for $2R_j=1.0$ mm, $U=2.754$ m/s.

B. Jet velocity profiles

In all the previous modeling efforts, it was assumed that the jet velocity is uniform at any jet cross section and the sheet velocity is the same as that of the jets $(u_s=U)$ because nothing caused the loss of jet momentum. However, the experimental measurement results of the jet velocity profile by Choo and Kang[15] definitely showed a nonuniform profile. Therefore, a nonuniform jet velocity profile should be considered in the prediction of the thickness and velocity of the liquid sheet.

The parabolic velocity profile of the jet in a circular cross section normal to the axis of the jet can be expressed as

$$u_j=Aq^2\sin^2\phi+A\sin^2\theta(q\cos\phi-b)^2+B \quad (3)$$

using the cylindrical coordinate system $f(q,\phi)$, where A is $(u_R-u_{\max})/R_j^2$ and B represents $u_{\max}$, the maximum velocity occurring at the center of the section. Once A and B are determined, the velocity profile of the jet in an elliptical cross section shown in Fig. 2(b) can be expressed in terms of $\{b,q,\phi,\theta\}$. For the case of uniform jet velocity, which was assumed in the previous theoretical predictions, both u_R and $u_{\max}$ are equal to the mean jet velocity U. For the case of Poiseuille parabolic velocity profile, which was assumed by Bremond and Villermaux,[6] $u_R=0$ and $u_{\max}=2U$.

The jet velocity profiles used for the theoretical predictions of the thickness and velocity of the sheet is shown in Fig. 3. Line ① is a uniform flow at $U=2.754$ m/s, and the dashed curve ② is a Poiseuille profile. The circle symbols ③ are the measured jet velocities using a laser Doppler velocimetry (LDV) and water as a test fluid by Choo and Kang,[15] which can be fitted using the parabolic equation (2) with $A=-9.377\times10^6$ 1/m s and $B=4.1723$ m/s, shown as curve ④. The mean velocity of the velocity profiles ② and ④ is equal to the uniform flow velocity, namely, $U=2.754$ m/s. The measured jet velocity profile ④ deviates much from the Poiseuille profile ② owing to the relaxation of parabolic velocity profile in a free jet, which depends on the preimpingement length of the jet (l). In their experimental measurements, the jet velocities across the jet were measured at a distance of $l/D_j=10$, namely, 10 mm from the exit of the glass tube of 1 mm inner diameter. The free jet diameter is increased over the initial jet diameter (1 mm), and the jet velocities near the boundary of a free jet are increased, and the maximum jet velocity at the center is decreased compared with the Poiseuille profile. In this study, three cases of jet velocity profiles, i.e., ①, ②, and ④, are considered to investigate the effect of initial jet velocity profile on the thickness and velocity characteristics of the liquid sheet.

C. Conservation equations

The basic concept used in deriving the conservation equations is that physical quantities such as mass, momentum, and energy are conserved between the angular element $d\phi$ of an elliptical section of the jet in Fig. 2(b) and the corresponding angular element $d\phi$ of the liquid sheet in Fig. 1. In this modeling, the effect of gravity and physical properties of liquid such as surface tension and viscosity is assumed to be negligible. Each conservation equation can be expressed as

(1) Mass conservation:

$$2\sin\theta d\phi\int_0^{q_j}qu_j dq=u_s hrd\phi, \quad (4)$$

(2) Momentum conservation:

$$\frac{2}{3}\pi R_j^2(u_R^2+u_Ru_{\max}+u_{\max}^2)\cos\theta=\int_0^{2\pi}u_s^2hr\cos\phi d\phi, \quad (5)$$

(3) Energy conservation:

$$2\sin\theta d\phi\int_0^{q_j}qu_j^3dq=u_s^3hrd\phi. \quad (6)$$

The left-hand sides of Eqs. (4) and (6) are the mass and energy fluxes of the two jets flowing through an angular

Downloaded 11 Nov 2007 to 168.131.132.191. Redistribution subject to AIP license or copyright, see http://pof.aip.org/pof/copyright.jsp

element $d\phi$ of an elliptical section of the jet in Fig. 2(b), and the right-hand sides are those flowing through the area $hrd\phi$ of the liquid sheet in Fig. 1. Similarly, the left-hand side of Eq. (5) represents the momentum of the two jets before impaction in the y direction and the right-hand side is the total momentum of the liquid sheet in the same y direction. The integral parts of Eqs. (4) and (6) are represented as $F\{b,q_j,\phi,\theta\}$ and $G\{b,q_j,\phi,\theta\}$, respectively. Using Eqs. (2) and (3), they are expressed as

$$F\{b,q_j,\phi,\theta\} = \int_0^{q_j} qu_j dq = \frac{1}{4}A(\cos^2\phi\sin^2\theta+\sin^2\phi)q_j^4 + \frac{2}{3}A\cos\phi\sin^2\theta bq_j^3 + \frac{1}{2}(A\sin^2\theta b^2+B)q_j^2, \tag{7}$$

$$G\{b,q_j,\phi,\theta\} = \int_0^{q_j} qu_j^3 dq = \frac{1}{8}A^3(\cos^2\phi\sin^2\theta+\sin^2\phi)^3q_j^8 - \frac{6}{7}A^3\cos\phi\sin^2\theta(\cos^2\phi\sin^2\theta+\sin^2\phi)^2bq_j^7 + \frac{1}{6}\{A^2(\cos^2\phi\sin^2\theta + \sin^2\phi)^2(B+A\sin^2\theta b^2) + 8A^3b^2\cos^2\phi\sin^4\theta(\cos^2\phi\sin^2\theta+\sin^2\phi) + A(\cos^2\phi\sin^2\theta+\sin^2\phi)[2A(B + A\sin^2\theta b^2)(\cos^2\phi\sin^2\theta+\sin^2\phi) + 4A^2\sin^4\theta\cos^2\phi b^2]\}q_j^6 - \frac{1}{5}\{8A^2b\sin^2\theta\cos\phi(\cos^2\phi\sin^2\theta+\sin^2\phi)^2(B + A\sin^2\theta b^2) - 2Ab\sin^2\theta\cos\phi[2(B+A\sin^2\theta b^2)(A\cos^2\phi\sin^2\theta+A\sin^2\phi) + 4A^2\sin^4\theta\cos^2\phi b^2]\}q_j^5 + \frac{1}{4}\{(B + A\sin^2\theta b^2)[2A(B+A\sin^2\theta b^2)(\cos^2\phi\sin^2\theta+A\sin^2\phi) + 4A^2\sin^4\theta\cos^2\phi b^2] + 8A^2b^2\cos^2\phi\sin^4\theta(B + A\sin^2\theta b^2)\}q_j^4 - 2Ab\cos\phi\sin^2\theta(B+A\sin^2\theta b^2)^2q_j^3 + \frac{1}{2}(B+A\sin^2\theta b^2)q_j^2. \tag{8}$$

Because the boundary of an ellipse (q_j) is a function of (b,θ,ϕ) in Eq. (2), the sheet velocity u_s and the thickness parameter K is expressed as

$$u_s\{b,\phi,\theta\} = (G/F)^{1/2}, \tag{9}$$

$$K\{b,\phi,\theta\} = hr = F^{3/2}/G^{1/2}. \tag{10}$$

D. Stagnation point

The variable b, which determines the position of the stagnation point in the liquid sheet, can be obtained from Eq. (5). The integrand u_s^2hr appearing in the integral part of Eq. (5) can be expressed as $u_s^2hr=(FG)^{1/2}$ using Eqs. (4) and (6). Because an analytical solution of Eq. (5) cannot be obtained, the values of b can be found after numerical integration.

Figure 4 shows the parameter b/R_j for the stagnation point as a function of the impingement angle θ. Curve ① is the case of uniform flow, and Hasson and Peck[4] showed that a simple relationship exists as

$$\frac{b}{R_j} = \beta\frac{1}{\tan\theta}, \tag{11}$$

where the proportional constant β is 1.0. Curve ② is the case of Poiseuille profile used by Bremond and Villermaux,[6] and the value of β is $\beta=0.68$. The result obtained by using the measured jet velocity profile is shown as curve ③, and the fitted curve using Eq. (11) is shown as curve ④. The value of β for this case is $\beta=0.849$, which is lower than that for the uniform flow ($\beta=1.0$) and higher than that for the Poiseuille flow ($\beta=0.68$). This result means that the value of β reduces as the difference between the maximum and minimum velocities of the jet increases, and it approaches 1 as the velocity profile becomes uniform.

III. COMPARISON WITH EXPERIMENTAL RESULTS

A. Thickness distribution

After the value of b is determined at an arbitrary value of the impingement angle θ, the thickness parameter K is obtained from Eq. (10), and the sheet thickness can be calculated by Eq. (1). Figure 5 compares the sheet thickness as a function of the azimuthal angle ϕ between theoretical predictions and experimental measurements. The measurements were conducted by Choo and Kang[12] using water as a test fluid at $\theta=60°$, $2R_j=0.8$ mm, $U=5.1$ m/s. Curves ①, ②, and ③ were obtained by theoretical predictions using uniform flow, Poiseuille profile, and measured jet velocity profile, respectively. Symbols in ④ represent the measurement results for $\phi<90°$; results for $\phi>90°$ were difficult to obtain.

In general, the liquid sheet is the thickest at $\phi=0°$, and the thickness decreases as ϕ increases. The uniform flow, which was the most commonly used in the previous analytical analysis, shows the maximum difference of the results from the experimental results at $\phi=0°$, and the sheet thickness is overestimated until around $\phi=80°$. On the contrary, the sheet thickness for the case of Poiseuille profile is always

Downloaded 11 Nov 2007 to 168.131.132.191. Redistribution subject to AIP license or copyright, see http://pof.aip.org/pof/copyright.jsp

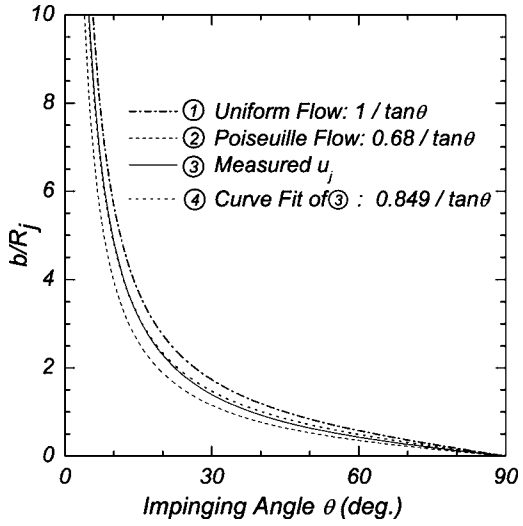

FIG. 4. Parameter b/R_j for the stagnation point as a function of the impinging angle θ.

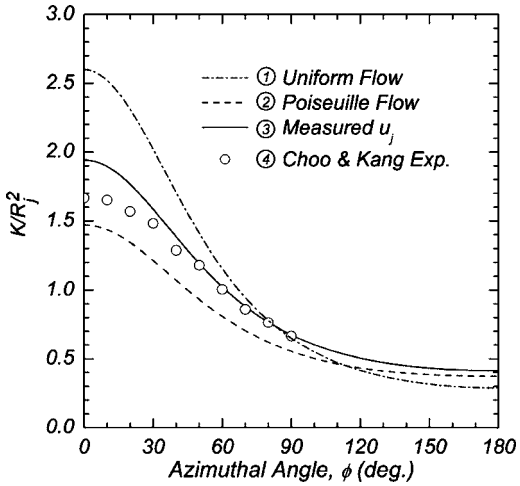

FIG. 5. Comparison of the thickness parameter between theoretical and experimental results.

lower than that measured experimentally. The sheet thickness using the measured jet velocity profile also shows a big difference from the experimental results at $\phi=0°$, where the sheet is the thickest, but the difference reduces as ϕ increases, where the sheet thickness decreases. Even though the measured jet velocity profile also showed some difference at $\phi=0°$, the thickness predicted by using it agreed best with the experimental results among three jet velocity profiles.

Figure 6 compares the maximum sheet thickness at $\phi=0°$ as a function of the impingement angle between theoretical predictions and experimental measurements conducted by Choo and Kang[12] at $2R_j=1.0$ mm, $U=3.0$ m/s. The uniform flow showed the largest difference from the experimental results but the Poiseuille flow agreed best with the measurements. As discussed in Fig. 5, the measured jet velocity profile showed the largest difference at $\phi=0°$. The prediction using it was worse than that using the Poiseuille flow, but better than that using the uniform flow. The difference became smaller as the impingement angle increased because the thickness decreased.

Based on the above results, the thickness predicted using uniform flow deviates most from the experimental results among the three profiles compared. The Poiseuille flow predicted the sheet thickness well when the sheet thickness was large, around $\phi=0°$ or at small impingement angles. The thickness predicted by the measured jet velocity profile agreed well with the experimental results when the sheet was thin with the increase of azimuthal or impingement angles.

B. Velocity distribution

Like the thickness prediction, the sheet velocity can be predicted by Eq. (9). Figure 7 compares the velocity distribution of the liquid sheet at different impingement angles as a function of the azimuthal angle ϕ between theoretical predictions and experimental measurements. The dotted and solid lines are obtained by theoretical predictions using the Poiseuille profile and the measured jet velocity profile, respectively. The symbols are the measurements obtained from experiments conducted by Choo and Kang[15] using water as a test fluid at $2R_j=1.0$ mm, $U=2.7$ m/s. Unlike the assumption in which the liquid sheet velocity is equal to the jet velocity U, in most of previous theoretical studies, the liquid sheet velocity definitely changes with respect to the azimuthal angle ϕ and the impingement angle θ when the jet velocity profile is considered. The sheet velocity for the case of Poiseuille profile was always higher than that measured experimentally, whereas the measured jet velocity profile always underestimated the sheet velocity. However, the difference of the sheet velocity between predictions using the measured jet velocity profile and the experimental results decreases as the impingement angle increases; this same tendency is observed with respect to the sheet thickness. On the contrary, the prediction using the Poiseuille profile becomes worse with the increase of the impingement angle.

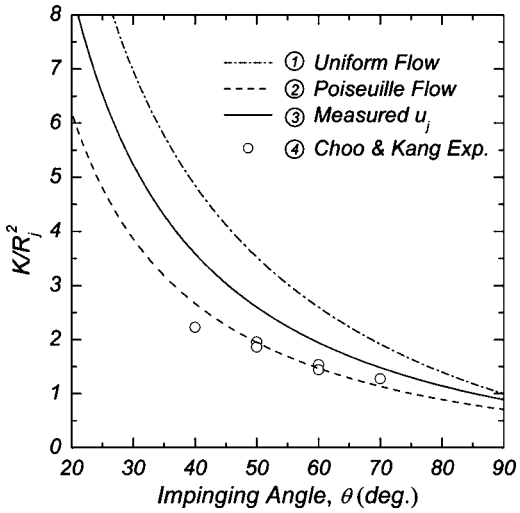

FIG. 6. Comparison of the thickness parameter between theoretical and experimental results as a function of the impinging angle at $\phi=0°$.

Downloaded 11 Nov 2007 to 168.131.132.191. Redistribution subject to AIP license or copyright, see http://pof.aip.org/pof/copyright.jsp

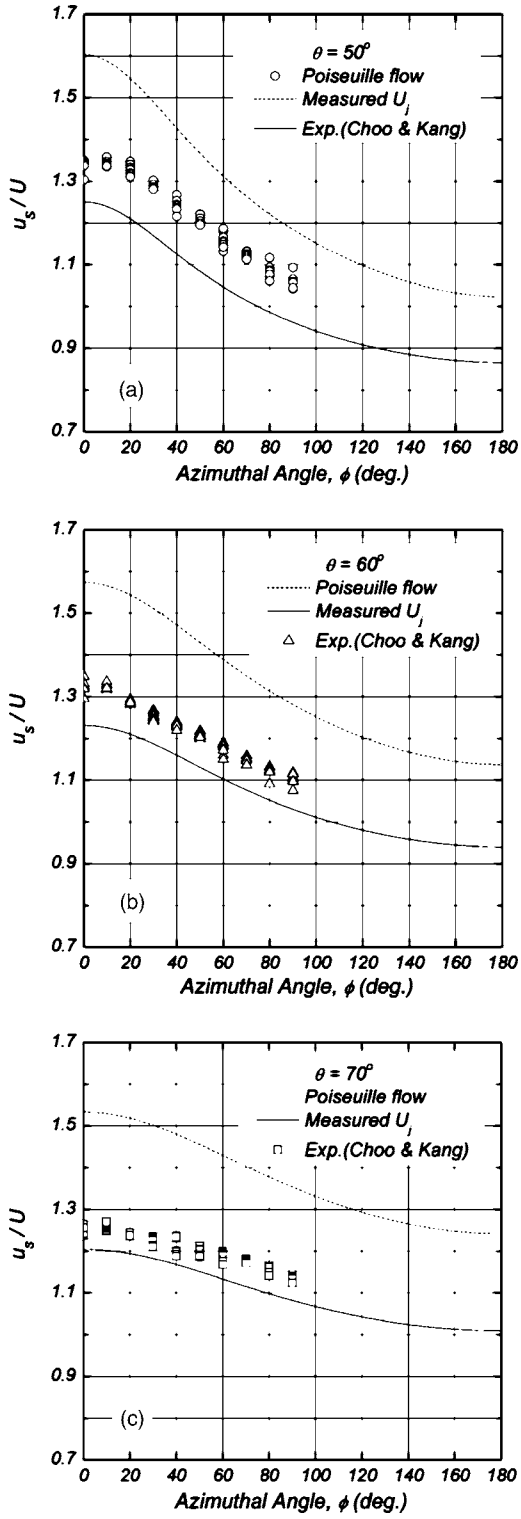

FIG. 7. Comparison of sheet velocity distribution between theoretical and experimental results: (a) θ=50°, (b) θ=60°, and (c) θ=70°.

C. Effect of other factors

Based on the comparison of the thickness and velocity of the liquid sheet between theoretical predictions and measurement results, the predictions considering the jet velocity profile produced more acceptable results, which agreed better with the experimental observations, than those using the constant jet velocity, which has been commonly used in previous theoretical works. Even though the theoretical predictions considering the jet velocity profile showed a close agreement with experimental results, there were noticeable differences between them. More refined theoretical predictions are necessary to reduce these differences. For example, the present theoretical predictions do not consider the effects of gravity or liquid properties. In the theoretical predictions, the liquid sheet was assumed to form in the plane normal to the direction of gravity so the effect of gravity can be neglected. However, for the case of the liquid sheet formed in the direction of gravity, gravity can assist the expansion of liquid, affecting the thickness and velocity of the liquid sheet. In Choo and Kang's thickness experiment,[12] the liquid sheet was formed in the direction of gravity, and the sheet was much thinner than the theoretical predictions possibly because of the effect of gravity. In addition, with experiments using glycerol solutions, they showed that the physical properties of the liquid such as surface tension and viscosity affected the resulting thickness of the liquid sheet. Therefore, additional studies on the theoretical predictions including the effects of gravity and physical properties of the liquid are required.

IV. CONCLUSIONS

In this study, the effect of jet velocity profile on the thickness and velocity of the liquid sheet formed by two impinging low-speed jets was investigated. To predict the distributions of the thickness and velocity of the liquid sheet theoretically, the jet velocity profile, which was measured experimentally by Choo and Kang,[15] was adopted in addition to the constant jet velocity and Poiseuille's parabolic profile. For three jet velocity profiles, the distributions of the thickness and velocity of the liquid sheet were analytically predicted by solving conservation equations for mass, momentum, and energy. The predicted results were compared with the previous experimental results. The jet velocity profile affected the resulting thickness and velocity characteristics of the liquid sheet. The distributions of the thickness and velocity of the liquid sheet predicted by using the measured jet velocity profile were closer to the measured results than those predicted by using the assumption of constant jet velocity.

[1] G. P. Sutton, *Rocket Propulsion Element: An Introduction to the Engineering of Rockets* (Wiley, New York, 1992), p. 298.
[2] W. E. Ranz, "Some experiments on the dynamics of liquid films," J. Appl. Phys. **30**, 1950 (1959).
[3] K. D. Miller, "Distribution of spray from impinging liquid jets," J. Appl. Phys. **31**, 1132 (1960).
[4] D. Hasson and R. E. Peck, "Thickness distribution in a sheet formed by impinging jets," AIChE J. **10**, 752 (1964).
[5] E. A. Ibrahim and A. J. Przekwas, "Impinging jets atomization," Phys. Fluids A **3**, 2981 (1991).
[6] N. Bremond and E. Villermaux, "Atomization by jet impact," J. Fluid Mech. **549**, 273 (2006).
[7] B. S. Kang, Y. B. Shen, and D. Poulikakos, "Holography experiments in the breakup region of a liquid sheet formed by two impinging jets," Atomization Sprays **5**, 387 (1995).
[8] H. S. Couto and D. Bastos-Netto, "Modeling droplet size distribution from

Downloaded 11 Nov 2007 to 168.131.132.191. Redistribution subject to AIP license or copyright, see http://pof.aip.org/pof/copyright.jsp

impinging jets," J. Propul. Power **7**, 654 (1991).
[9]F. R. S. Taylor, "Formation of thin flat sheets of water," Proc. R. Soc. London, Ser. A **259**, 1 (1960).
[10]Y. B. Shen, Ph.D. thesis, Department of Mechanical Engineering, University of Illinois at Chicago, 1997.
[11]Y. B. Shen and D. Poulikakos, "Thickness variation of liquid sheet formed by two impinging jets using holographic interferometry," J. Fluids Eng. **120**, 482 (1998).
[12]Y. J. Choo and B. S. Kang, "Parametric study on impinging-jet liquid sheet thickness distribution using an interferometric method," Exp. Fluids **31**, 56 (2001).
[13]R. Li and N. Ashgriz, "Characteristics of liquid sheets formed by two impinging jets," Phys. Fluids **18**, 087104 (2006).
[14]N. Dombrowski and P. C. Hooper, "A study of the sprays formed by impinging jets in laminar and turbulent flow," J. Fluid Mech. **18**, 392 (1963).
[15]Y. J. Choo and B. S. Kang, "The velocity distribution of the liquid sheet formed by two low-speed impinging jets," Phys. Fluids **14**, 622 (2002).
[16]J. D. Naber and R. D. Reitz, "Modeling engine spray/wall impingement," SAE 880107 (1988).

Downloaded 11 Nov 2007 to 168.131.132.191. Redistribution subject to AIP license or copyright, see http://pof.aip.org/pof/copyright.jsp